

Significance of the hydrophobic residues 225–230 of apoA-I for the biogenesis of HDL¹

Panagiotis Fotakis,^{*,†} Ioanna Tiniakou,[†] Andreas K. Kateifides,^{*,†} Christina Gkolfinopoulou,[§] Angeliki Chroni,[§] Efstratios Stratikos,[§] Vassilis I. Zannis,^{2,3,*,†} and Dimitris Kardassis^{2,†}

Whitaker Cardiovascular Institute,* Boston University School of Medicine, Boston, MA 02118; Department of Biochemistry,[†] University of Crete Medical School, Heraklion, Crete, Greece 71110; and National Center for Scientific Research “Demokritos”,[§] Athens, Greece 15310

Abstract We studied the significance of four hydrophobic residues within the 225–230 region of apoA-I on its structure and functions and their contribution to the biogenesis of HDL. Adenovirus-mediated gene transfer of an apoA-I[F225A/V227A/F229A/L230A] mutant in apoA-I^{-/-} mice decreased plasma cholesterol, HDL cholesterol, and apoA-I levels. When expressed in apoA-I^{-/-} × apoE^{-/-} mice, approximately 40% of the mutant apoA-I as well as mouse apoA-IV and apoB-48 appeared in the VLDL/IDL/LDL. In both mouse models, the apoA-I mutant generated small spherical particles of pre- β - and α 4-HDL mobility. Coexpression of the apoA-I mutant and LCAT increased and shifted the-HDL cholesterol peak toward lower densities, created normal α HDL subpopulations, and generated spherical-HDL particles. Biophysical analyses suggested that the apoA-I[225–230] mutations led to a more compact folding that may limit the conformational flexibility of the protein. The mutations also reduced the ability of apoA-I to promote ABCA1-mediated cholesterol efflux and to activate LCAT to 31% and 66%, respectively, of the WT control. Overall, the apoA-I[225–230] mutations inhibited the biogenesis of-HDL and led to the accumulation of immature pre- β - and α 4-HDL particles, a phenotype that could be corrected by administration of LCAT.—Fotakis, P., I. Tiniakou, A. K. Kateifides, C. Gkolfinopoulou, A. Chroni, E. Stratikos, V. I. Zannis, and D. Kardassis. **Significance of the hydrophobic residues 225–230 of apoA-I for the biogenesis of HDL.** *J. Lipid Res.* 2013. 54: 3293–3302.

Supplementary key words apolipoprotein A-I mutations • high density lipoprotein biogenesis • pre- β - and α -HDL particles • dyslipidemia

Previous studies by us showed the overall importance of the 220–231 region of apoA-I for apoA-I/ABCA1 interactions

This work was supported by National Institutes of Health Grant HL-48739; General Secretariat of Research and Technology of Greece Grant Synergasia 09SYN-12-897 (to D.K. and A.C.); and Ministry of Education of Greece Grant Thalys MIS 377286 (to D.K., A.C., and E.S.). P. Fotakis has been supported by pre-doctoral training Fellowship HERACLEITUS II by the European Union and Greek national funds through the Operational Program “Education and Lifelong Learning” of the National Strategic Reference Framework (NSRF).

Manuscript received 27 August 2013 and in revised form 9 October 2013.

Published, *JLR Papers in Press*, October 12, 2013
DOI 10.1194/jlr.M043489

Copyright © 2013 by the American Society for Biochemistry and Molecular Biology, Inc.

This article is available online at <http://www.jlr.org>

and the biogenesis of HDL but did not identify the apoA-I residues involved (1, 2). Other studies also showed the importance of the C-terminal region for the structure of apoA-I (3–5) as well as for other functions of apoA-I (6, 7). In the preceding article, we investigated the role of the hydrophobic residues L218, L219, V221, and L222 and the charged residues E223 and K226 on the structure and functions of apoA-I and their contribution to the biogenesis of HDL (8). These studies showed that substitution of the hydrophobic residues L218, L219, V221, and L222 of apoA-I by alanines inhibits the biogenesis and maturation of HDL and generates a phenotype that cannot be corrected by LCAT. Expression of E223 and K226 caused fewer but discrete alterations in the HDL phenotype.

The rationale for the present study was that the 225–230 region of apoA-I contains four additional hydrophobic residues that may be equally significant for its structure and functions. For this reason, we used gene transfer in two mouse models as well as biochemical and biophysical analyses to study the impact of substitutions of residues F225, V227, F229, and L230 by alanines on the structure and functions of apoA-I and their impact on the biogenesis of HDL. In vitro experiments showed that the apoA-I[225–230] mutations affected the structure of apoA-I, diminished its capacity to promote ABCA1-mediated cholesterol efflux, and decreased moderately its ability to activate LCAT. Gene transfer of the apoA-I mutant in apoA-I^{-/-} and apoA-I^{-/-} × apoE^{-/-} mice resulted in the reduction

Abbreviations: ANS, 8-anilino-1-naphthalene-sulfonate; CD, circular dichroism; DMPC, dimyristoyl-L- α -phosphatidylcholine; EM, electron microscopy; FPLC, fast-protein liquid chromatography; GdnHCl, guanidine hydrochloride; HEK293, human embryonic kidney 293; HTB-13, SW 1783 human astrocytoma; POPC, β -oleoyl- γ -palmitoyl-L- α -phosphatidylcholine; WMF, wavelength of maximum fluorescence; WT, wild-type.

¹See referenced companion article, *J. Lipid Res.* 2013, 54: 3281–3292.

²V. I. Zannis and D. Kardassis contributed equally to this work.

³To whom correspondence should be addressed.

e-mail: vzannis@bu.edu

■ The online version of this article (available at <http://www.jlr.org>) contains supplementary data in the form of one table, three figures, and methods.

of plasma apoA-I and HDL levels and led to the formation of spherical particles with pre- β - and α 4-HDL electrophoretic mobility. In contrast to the apoA-I[218–222] mutant described in the preceding article (8), the defective HDL phenotype caused by the 225–230 mutations could be corrected by coexpression of the apoA-I mutant and human LCAT.

MATERIALS AND METHODS

Materials

Materials not mentioned in the experimental procedures have been obtained from sources described previously (9, 10).

Generation of adenoviruses expressing the wild-type and mutant apoA-I forms

The apoA-I gene lacking the BglII restriction site, which is present at nucleotide position 181 of the genomic sequence relative to the ATG codon of the gene, was cloned into the pCDNA3.1 vector to generate the pCDNA3.1-apoA-I(Δ BglII) plasmid as described (11). This plasmid was used as a template to introduce the apoA-I mutations F225A/V227A/F229A/L230A using the QuickChange® XL mutagenesis kit (Stratagene, Santa Clara, CA) and the mutagenic primers shown in supplementary Table I. Recombinant adenoviruses expressing the WT and the mutant apoA-I were constructed using the Ad-Easy-1 system in which the recombinant adenovirus construct is generated in bacteria BJ-5183 (purchased from Stratagene) (12). The recombinant adenovirus was packaged in 911 cells, amplified in human embryonic kidney 293 (HEK 293) cells, purified, and titrated as described (11).

ApoA-I production, purification, ABCA1-dependent cholesterol efflux and LCAT assays, physicochemical measurements, animal studies, and statistics were described in the preceding article (8).

RESULTS

Secretion of the WT and the apoA-I[225–230] mutant in the culture media of cells

The secretion of WT and mutant form of apoA-I in the culture medium of HTB-13 cells expressing the WT and the mutant apoA-I form was assessed by SDS-PAGE analysis of the culture media. As shown in supplementary Fig. 1, both the WT and the apoA-I[225–230] mutant were secreted

at comparable levels in the culture medium of the apoA-I-expressing cells.

Expression of the apoA-I transgenes following adenovirus infection

Total hepatic RNA was isolated from the livers of apoA-I^{-/-} or apoA-I^{-/-} × apoE^{-/-} mice four days post infection with adenoviruses expressing the WT apoA-I and the apoA-I[225–230] mutant. qRT-PCR analysis of the apoA-I mRNA levels showed that the expression of the apoA-I[225–230] mutant was comparable to WT apoA-I in apoA-I^{-/-} × apoE^{-/-} mice but slightly elevated in apoA-I^{-/-} mice (Table 1).

Plasma lipid and apoA-I levels and FPLC profiles

Plasma lipids and apoA-I levels were determined four days post infection of apoA-I^{-/-} or apoA-I^{-/-} × apoE^{-/-} mice with adenoviruses expressing the WT and the mutant apoA-I form. It was found that in apoA-I^{-/-} mice the apoA-I[225–230] mutant decreased plasma cholesterol and apoA-I levels to 23% and 34%, respectively, as compared with WT apoA-I. Plasma triglycerides were not affected by the apoA-I mutations (Table 1). Fast-protein liquid chromatography (FPLC) analysis of plasma from apoA-I^{-/-} mice infected with the recombinant adenovirus expressing either WT apoA-I or the apoA-I[225–230] mutant showed that all the cholesterol was distributed in the HDL region and that the HDL cholesterol peak of the apoA-I[225–230] mutant was greatly diminished (Fig. 1A).

Fractionation of plasma of apoA-I^{-/-} mice expressing the WT apoA-I or the apoA-I[225–230] mutant, EM analysis, and two-dimensional electrophoresis

Fractionation of plasma by density gradient ultracentrifugation and subsequent analysis of the resulting fractions by SDS-PAGE showed that both the WT apoA-I and the apoA-I[225–230] mutant were predominantly distributed in the HDL3 region and to a lesser extent in the HDL2 region (Fig. 1B, C). Compared with WT apoA-I, the quantity of the apoA-I[225–230] mutant was greatly reduced (Fig. 1B, C). Flotation of other apolipoproteins in the VLDL/LDL/IDL/HDL region was not observed when the WT apoA-I and the apoA-I[225–230] mutant were expressed in apoA-I^{-/-} mice.

TABLE 1. Plasma lipids, apoA-I, and hepatic mRNA levels of apoA-I^{-/-} or apoA-I^{-/-} × apoE^{-/-} mice expressing WT and the mutant form of apoA-I as indicated

Treatment	None	WT ApoAI	ApoA-I[225–230]	ApoA-I[225–230] + LCAT
ApoAI ^{-/-} mice				
ApoA-Ih mRNA levels (%)	Nondetectable	100 ± 15 ^a	130 ± 10 ^b	80 ± 10
Plasma apoA-Ih protein (mg/dl)	Nondetectable	173 ± 63	59 ± 17 ^c	149 ± 43
Plasma cholesterol (mg/dl)	27 ± 8	182 ± 82 ^d	41 ± 12 ^{d,e}	297 ± 69 ^d
Plasma triglycerides (mg/dl)	34 ± 14	39 ± 15	42 ± 14	48 ± 21
ApoAI ^{-/-} × apoE ^{-/-} mice				
ApoA-Ih mRNA levels (%)	Nondetectable	100 ± 21 ^a	140 ± 50	90 ± 30
TC (mg/dl)	337 ± 107	520 ± 85	377 ± 90	778 ± 103 ^{d,e}
TG (mg/dl)	58 ± 23	680 ± 290 ^d	35 ± 22 ^e	87 ± 65 ^e

Values are means ± SD based on analysis of 5–8 mice per experiment.

^a Expression of WT apoA-I in the apoA-I^{-/-} or apoA-I^{-/-} × apoE^{-/-} was set to 100%. Expression of LCAT was also confirmed by RT-PCR. Statistical significant differences at $P < 0.05$ were calculated between untreated mice and mice expressing the WT apoA-I and the apoA-I[F225A/V227A/F229A/L230A] in either the apoA-I^{-/-} or apoA-I^{-/-} × apoE^{-/-} mouse background and are indicated as follows: ^b $P \leq 0.05$ relative to WT apoA-I control; ^c $P \leq 0.05$ relative to WT apoA-I control; ^d $P \leq 0.05$ relative to the untreated control; ^e $P \leq 0.05$ relative to WT apoA-I control.

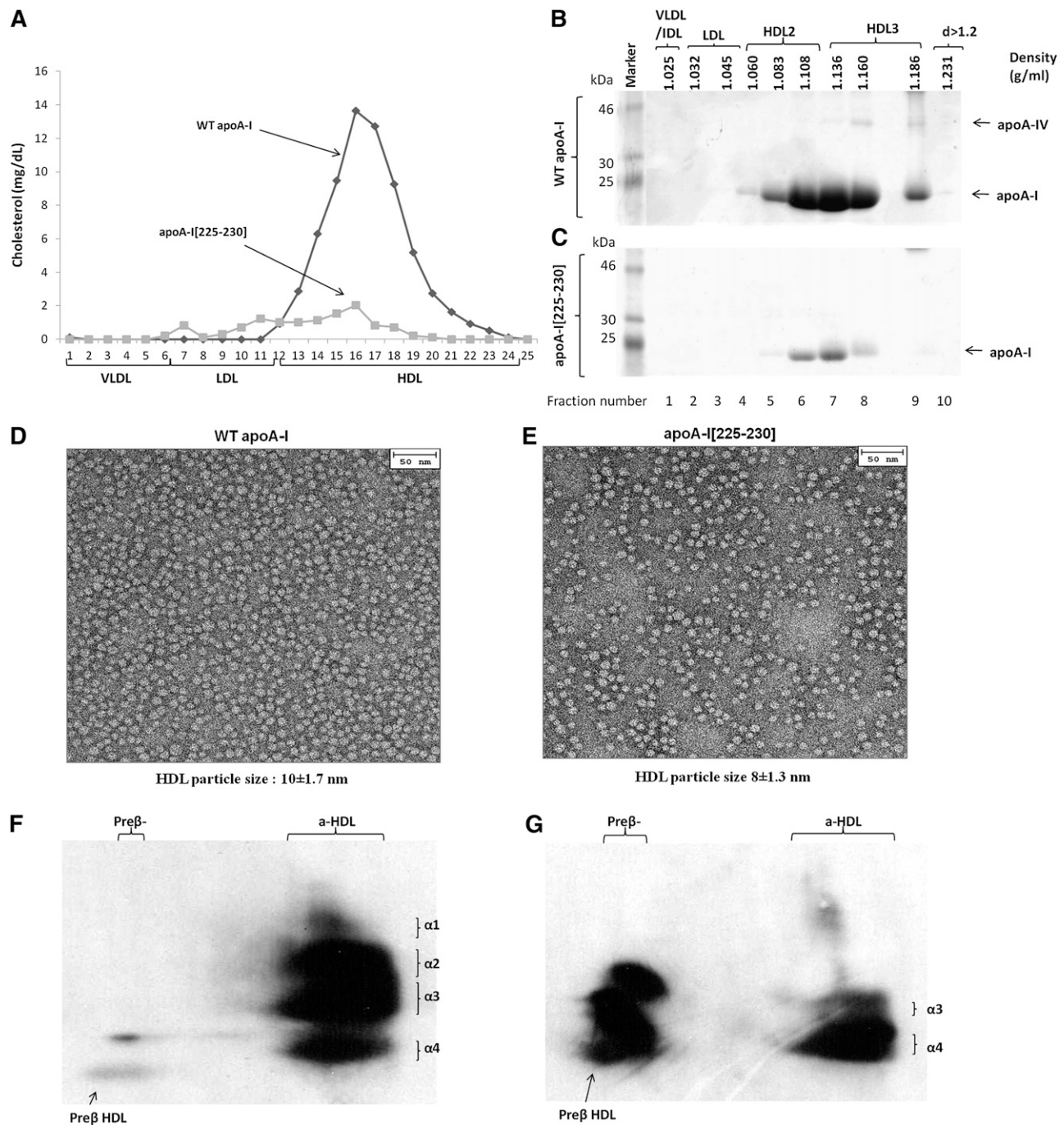


Fig. 1. Analysis of plasma of apoA-I^{-/-} mice infected with adenoviruses expressing the WT apoA-I or apoA-I[225–230] by FPLC (A) and by density gradient ultracentrifugation and SDS-PAGE (B, C). EM analysis of HDL fractions 6 and 7 obtained from apoA-I^{-/-} mice expressing the WT apoA-I (D) or apoA-I[225–230] mutant (E) following density gradient ultracentrifugation of plasma as indicated. The photomicrographs in this as well as in Figs. 2 and 3 were taken at 75,000 \times magnification and enlarged three times. The average diameter of the particles in this as well as in Figs. 2 and 3 was determined by measuring the diameter of 200 individual particles. Two-dimensional gel electrophoresis of plasma of apoA-I^{-/-} mice infected with adenoviruses expressing WT apoA-I (F) or apoA-I[225–230] mutant (G).

Analysis of the HDL fractions 6 and 7 obtained following density gradient ultracentrifugation by EM showed that both the WT apoA-I and the apoA-I[225–230] mutant generated spherical particles (Fig. 1D, E). The diameters of the particles were 10 ± 1.7 nm for the WT apoA-I and 8 ± 1.3 nm for the apoA-I[225–230] mutant. Two-dimensional gel electrophoresis of plasma showed that WT apoA-I formed normal pre- β and α 1, α 2, α 3, α 4-HDL subpopulations (Fig. 1F),

whereas the apoA-I[225–230] mutant formed predominantly pre- β and α 4 subpopulations (Fig. 1G).

To assess how apoE deficiency affects HDL biogenesis, we also performed gene transfer experiments in apoA-I^{-/-} \times apoE^{-/-} mice, which lack both mouse apoA-I and apoE. The plasma cholesterol and triglyceride levels of mice expressing the apoA-I[225–230] mutant were comparable to those of the noninfected apoA-I^{-/-} \times apoE^{-/-} mice (Table 1).

In contrast, the plasma cholesterol levels of the mice expressing the WT apoA-I were increased 1.5-fold compared with the uninfected apoA-I^{-/-} × apoE^{-/-} mice, and the apoA-I expressing mice developed hypertriglyceridemia. The difference in the plasma cholesterol levels between apoA-I^{-/-} × apoE^{-/-} mice expressing WT apoA-I and the apoA-I[225–230] mutant can be explained by the corresponding FPLC analyses of the plasmas. This analysis showed that in apoA-I^{-/-} × apoE^{-/-} mice expressing the WT apoA-I, approximately two thirds of the cholesterol was found in the VLDL/IDL region and the remaining in the HDL region. In contrast, in mice expressing the apoA-I[225–230] mutant, the great majority of the cholesterol (>90%) was found in the VLDL/IDL region and the remaining in the LDL region. There was no appreciable HDL cholesterol peak in the HDL region (Fig. 2A). All triglycerides were found in the VLDL/IDL region (Fig. 2B).

Fractionation of the plasma by density gradient ultracentrifugation showed that WT apoA-I was distributed predominantly in the HDL2/HDL3 region, with small amounts in the VLDL/IDL/LDL region (Fig. 2C). Similar analysis for the apoA-I[225–230] mutant showed that apoA-I and mouse apoA-IV were distributed in all lipoprotein fractions and that the VLDL/IDL/LDL/HDL2 fractions were enriched with mouse apoB-48 (Fig. 2D). EM analysis of the fractions 6 and 7 obtained by density gradient ultracentrifugation of the plasma showed that both the WT apoA-I and the apoA-I mutant generated spherical particles that differed in size (Fig. 2E, F). The diameter of the particles were 9.2 ± 1.9 nm for the WT apoA-I and 7 ± 2.3 for the apoA-I[225–230] mutant. Larger spherical particles corresponding in size to IDL and LDL were observed in the HDL density fractions of apoA-I^{-/-} × apoE^{-/-} mice expressing the apoA-I[225–230] mutant. The appearance of the IDL- and LDL-sized particles coincides with the presence of apoB-48 in fractions 6 and 7 used for the EM analysis (Fig. 2D). Two-dimensional gel electrophoresis showed that the plasma of mice expressing WT apoA-I contained the normal pre-β and α-HDL subpopulations (Fig. 2G), whereas the plasma of mice expressing the apoA-I[F225A/V227A/F229A/L230A] mutant contained predominantly (~70%) pre-β, smaller amounts of (~30%) of α4-HDL, and few α3-HDL particles (Fig. 2H). The relative migration of the particles generated by WT apoA-I and the apoA-I[225–230] mutant in apoA-I^{-/-} and apoA-I^{-/-} × apoE^{-/-} mice were established by two-dimensional gel electrophoresis of mixtures of the plasmas containing these two apoA-I forms (supplementary Fig. II-A, B).

To assess whether the defective phenotype of the apoA-I[225–230] mutant can be corrected by LCAT, we carried out gene transfer of both the apoA-I[225–230] mutant and LCAT in apoA-I^{-/-} and apoA-I^{-/-} × apoE^{-/-} mice. In apoA-I^{-/-}, the coexpression of the apoA-I[225–230] mutant and LCAT increased plasma cholesterol without changing the plasma triglyceride levels (Table 1). The FPLC analysis of the plasma showed that the increase in plasma cholesterol was accompanied by a dramatic increase in the HDL cholesterol peak and its shift toward the lower densities (Fig. 3A). In double-deficient mice, the coexpres-

sion of the apoA-I[225–230] mutant with LCAT caused a 2.3-fold increase in plasma cholesterol compared with noninfected mice, without any significant change in plasma triglycerides (Table 1). The FPLC analysis showed that the increase in plasma cholesterol was associated with the generation of a cholesterol shoulder that extended from VLDL to HDL (Fig. 3B). Density gradient ultracentrifugation of plasma in apoA-I^{-/-} mice coexpressing the apoA-I[225–230] mutant and LCAT showed that the major proportion of apoA-I was distributed mainly in the HDL2 region and a smaller amount in the VLDL/IDL/LDL and HDL3 regions. Mouse apoE was distributed predominantly in the VLDL/IDL/LDL region and to a lesser extent in the HDL2 region. Mouse apoA-IV floated in all lipoprotein fractions (Fig. 3C). The identity of the apoA-IV and apoE bands was confirmed by western blotting (data not shown). In apoA-I^{-/-} × apoE^{-/-} mice expressing both the apoA-I[225–230] mutant and LCAT, both apoA-I and apoA-IV were distributed in all lipoprotein fractions. ApoB-48 was present predominantly in the VLDL/IDL/LDL and HDL2 region and to a lesser extent in the HDL3 region (Fig. 3D). Electron microscopy of the HDL fractions 6 and 7 obtained from the plasma of apoA-I^{-/-} mice coexpressing the apoA-I[225–230] mutant and LCAT showed the presence of spherical particles of 11 ± 3.1 nm diameter (Fig. 3E). Similar analysis of the HDL fractions 6 and 7 of plasma of apoA-I^{-/-} × apoE^{-/-} mice coexpressing the apoA-I[225–230] mutant and LCAT also showed the presence of spherical particles of 10.3 ± 2.8 nm diameter as well as a greater proportion of the larger particles that correspond in size to VLDL/IDL/LDL size (Fig. 3F). Two-dimensional gel electrophoresis of plasma of both apoA-I^{-/-} and apoA-I^{-/-} × apoE^{-/-} mice showed that the coexpression of the apoA-I[225–230] mutant with LCAT restored the normal pre-β and α-HDL subpopulations and generated αHDL size subpopulations with larger size (Fig. 3G, H).

Comparative analysis of the in vitro functions and physicochemical properties of the WT apoA-I and the apoA-I[225–230] mutant

The WT apoA-I and the apoA-I[225–230] mutant were purified from the culture media of HTB-13 cells expressing the corresponding proteins and used for in vitro functional and physicochemical studies. The functional studies showed that the ability of this mutant to promote ABCA1-mediated cholesterol efflux and to activate LCAT was 31% and 66%, respectively, as compared with the WT control (Fig. 4A, B).

Circular dichroism (CD) measurements indicated 7.6% loss of helical content in the apoA-I[225–230] mutant (Table 2 and supplementary Fig. III-A). Thermal unfolding followed by the CD signal showed that the F225A/V227A/F229A/L230A mutations caused a more cooperative unfolding transition as compared with WT apoA-I (Table 2 and supplementary Fig. III-B). In contrast, the chemical unfolding profile of the mutant, probed by the intrinsic tryptophan fluorescence, was similar to that of the WT apoA-I (Table 2 and supplementary Fig. III-C). Finally, the ANS fluorescence measurements showed that

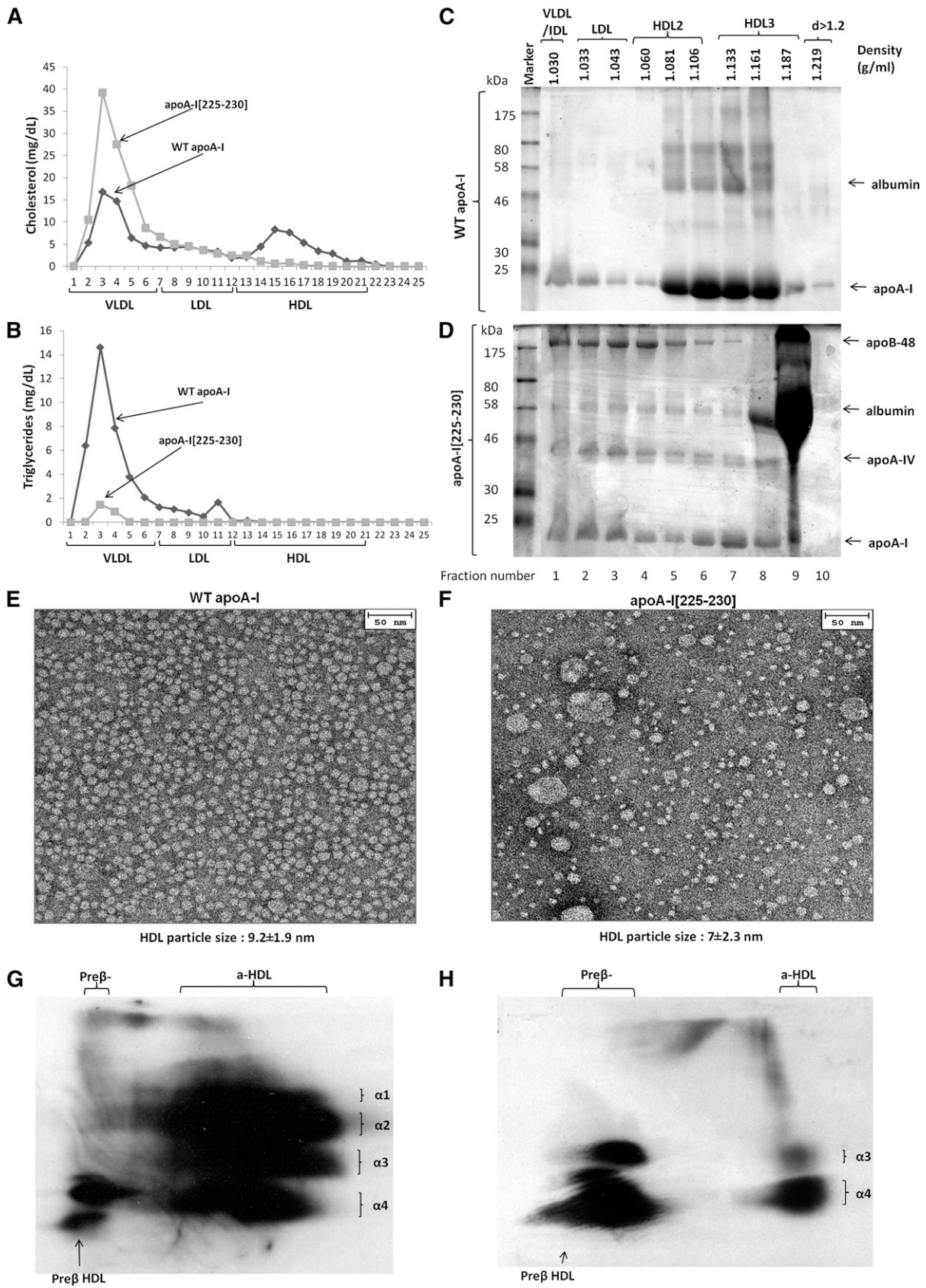


Fig. 2. Analysis of plasma of apoA-I^{-/-} × apoE^{-/-} mice infected with adenoviruses expressing the WT apoA-I or apoA-I[225–230] mutant by FPLC (A, B) and by density gradient ultracentrifugation and SDS-PAGE (C, D). EM analysis of HDL fractions 6 and 7 obtained from apoA-I^{-/-} × apoE^{-/-} mice expressing the WT apoA-I (E) or apoA-I[225–230] mutant (F) following density gradient ultracentrifugation of plasma as indicated. Two-dimensional gel electrophoresis of plasma of apoA-I^{-/-} × apoE^{-/-} mice infected with adenoviruses expressing WT apoA-I (G) or apoA-I[225–230] mutant (H).

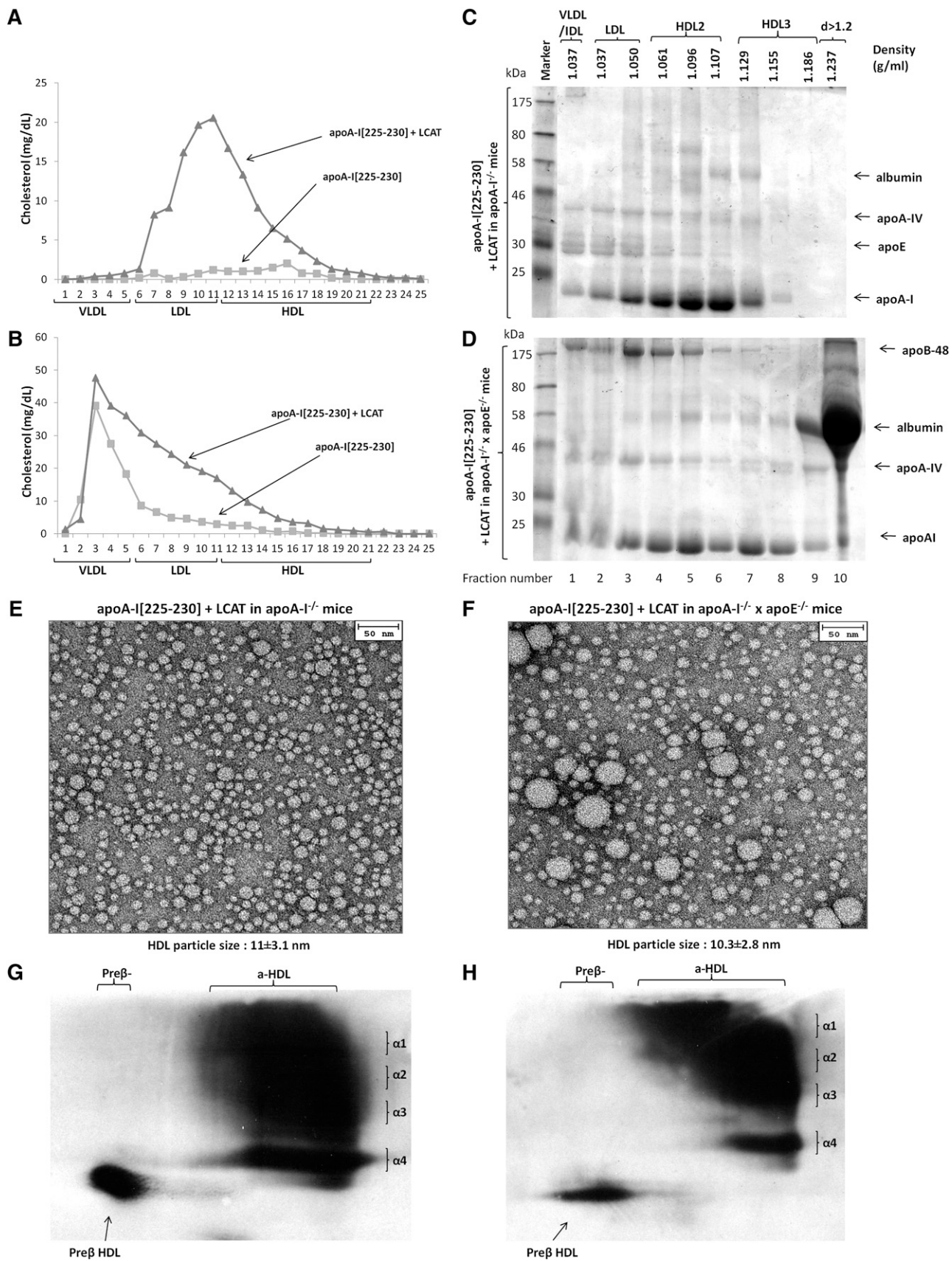


Fig. 3. Analyses of plasma of apoA-I^{-/-} (A,C,E,G) or apoA-I^{-/-} x apoE^{-/-} mice (B, D, F, H) infected with adenoviruses expressing the apoA-I[225-230] mutant in combination with human LCAT. Plasma FPLC profiles of mice expressing the apoA-I[225-230] mutant alone or the apoA-I[225-230] mutant in combination with human LCAT in apoA-I^{-/-} (A) or apoA-I^{-/-} x apoE^{-/-} background (B). SDS-PAGE of fractions obtained by density gradient ultracentrifugation from apoA-I^{-/-} (C) or apoA-I^{-/-} x apoE^{-/-} mice (D) mice expressing the apoA-I[225-230]

the F225A/V227A/F229A/L230A mutations caused a 41% reduction of hydrophobic surface exposure to the solvent (Table 2 and supplementary Fig. III-D).

DISCUSSION

F225A/V227A/F229A/L230A mutations alter the functional and physicochemical properties of apoA-I

The functional assays probed two well-characterized properties of lipid-free and lipoprotein-bound apoA-I, which are its ability to promote ABCA1-mediated cholesterol efflux and to activate LCAT, respectively (1, 13, 14). The decreased capacity of the apoA-I[225–230] mutant to promote ABCA1-mediated cholesterol efflux (31% of the WT control) is expected to influence its capacity to form HDL in vivo. The reduction in the ability of the apoA-I mutant to activate LCAT was modest (65% of WT control). However, previous studies showed that the capacity of reconstituted HDL containing an apoA-I mutant to activate LCAT in vitro does not always predict their ability to affect LCAT activation in vivo (15, 16).

The physicochemical analysis of the apoA-I[225–230] mutant suggested that the mutations lead to a more compact folding that may limit the conformational flexibility of the protein. The observed 7.6% decrease in the protein's α -helical content indicated that the structural changes brought about by the mutations extend beyond the limited area of the location of the mutations. Thermodynamic stability analysis indicated that the mutation also resulted in a protein that is thermodynamically stabilized and presents a more cooperative unfolding transition and compact structure. This was only evident during thermal unfolding and not during chemical denaturation. Since, however, the chemical denaturation reports only on the local environment of the tryptophan residues of the protein, which are all located on the N-terminal region of apoA-I, this observation suggests that the structural repercussions brought about by the mutations may be limited to the C-terminal region of apoA-I where the mutation resides. In either case, a more cooperative thermal transition signifies a more compact structure with reduced conformational flexibility, a property that is necessary for lipid association. A recent, related study involving different amino acid substitutions within the 225–236 region of apoA-I explored the effects of the aromatic and hydrophobic residues F225, F229, A232, and Y236 on the cholesterol efflux capacity and the ability of apoA-I to solubilize phospholipids and form HDL particles by cell cultures. It was concluded that both functions were similar to those of WT apoA-I when the overall hydrophobicity of apoA-I was not affected by the mutations in residues F225, F229, A232, and Y236. However, both functions were impeded by a factor of three by substitution of the aromatic amino acids that decreased the hydrophobicity of apoA-I (17). Another important finding of the present study is that although F225/V227/F229/L230 represent

~5% of total hydrophobic amino acids of apoA-I, their substitution by alanines resulted in a 41% reduction in the ANS fluorescence, indicating that these residues constitute a major solvent-exposed hydrophobic patch on the surface of apoA-I. Overall, our findings suggest that the F225A/V227A/F229A/L230A mutations greatly affect the structural integrity and conformational flexibility of apoA-I, effects that may at least partially underlie the observed changes in its in vitro and in vivo functions.

225–230 mutations are associated with abnormalities in the biogenesis and maturation of HDL

In previous studies, systematic mutagenesis and gene transfer of human apoA-I mutants in apoA-I-deficient mice disrupted specific steps along the pathway of the biogenesis of HDL and generated discrete HDL phenotypes (16). These phenotypes were characterized by low HDL levels, preponderance of immature HDL subpopulations, or accumulation of discoidal HDL particles in plasma (1, 10, 11, 15, 18, 19).

To obtain a clearer picture how the apoA-I mutations affected different steps of the biogenesis and maturation of HDL in the presence or absence of the endogenous mouse apoE, gene transfer studies were carried out in apoA-I^{-/-} mice that lack mouse apoA-I and in apoA-I^{-/-} × apoE^{-/-} mice that lack both mouse apoA-I and apoE.

The studies in apoA-I^{-/-} mice showed that the expression of the apoA-I[225–230] mutant was associated with a great reduction in the plasma cholesterol and apoA-I levels, despite the fact that the expression of the mutant transgene was higher than that of the WT apoA-I transgene. The reduction in plasma apoA-I was associated with a great decrease in the HDL cholesterol levels as determined by FPLC fractionation of the plasma and was further confirmed by density gradient ultracentrifugation of plasma, which showed reduction in the quantity of the apoA-I[225–230] mutant.

Potential abnormalities in the HDL phenotype in apoA-I^{-/-} mice resulting from the expression of the apoA-I[225–230] mutant were verified by two-dimensional gel electrophoresis of plasma that showed the formation of pre- β - and α 4-HDL particles. Accumulation of such particles is indicative of defective maturation of HDL due to insufficiency of mouse LCAT (11, 18). The LCAT insufficiency may originate from fast catabolism of the nascent HDL particles along with the endogenous LCAT bound to them (11). Fast catabolism of the nascent HDL particles by the kidney has been described previously (18, 20).

The plasma of both of apoA-I^{-/-} and apoA-I^{-/-} × apoE^{-/-} mice expressing the apoA-I[225–230] mutant contained predominantly pre- β - and, to a lesser extent, α 4-HDL particles, thus reaffirming the concept that the apoA-I[225–230] mutations affected the biogenesis of HDL. An unexpected finding was that the expression of the apoA-I[225–230] mutant in apoA-I^{-/-} × apoE^{-/-} mice resulted in the flotation of the mutant protein in all density fractions, along with mouse apoA-IV and apoB-48. The

mutant and human LCAT. EM analysis of HDL fractions 6 and 7 obtained from apoA-I^{-/-} (E) or apoA-I^{-/-} × apoE^{-/-} (F) mice expressing the apoA-I[225–230] mutant and human LCAT following density gradient ultracentrifugation of plasma as indicated. Two-dimensional gel electrophoresis of plasma of apoA-I^{-/-} (G) or apoA-I^{-/-} × apoE^{-/-} (H) mice expressing the apoA-I[225–230] mutant and human LCAT.

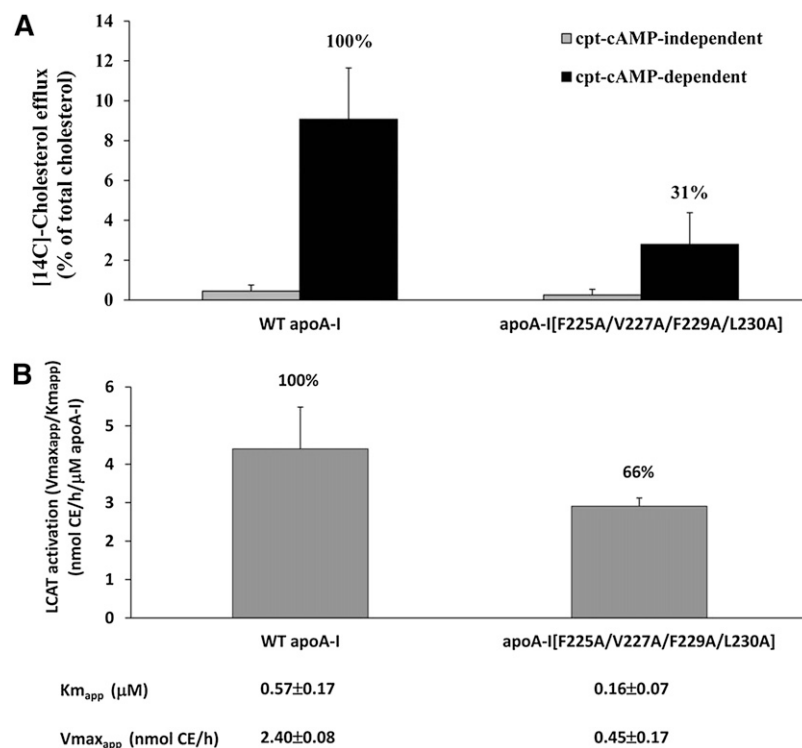


Fig. 4. ABCA1-mediated cholesterol efflux from J774 mouse macrophages treated with cpt-cAMP using WT apoA-I and the apoA-I[225–230] mutant as cholesterol acceptors (A). LCAT activation capacity of WT apoA-I and the apoA-I[225–230] mutant. Experiments were performed as described in Materials and Methods. The data represent the average from two independent experiments performed in triplicate (B).

presence of apoB-48 in the higher density fractions affected the particle composition of the HDL fraction by enriching it with larger particles corresponding in size to VLDL, IDL, and LDL. Previous studies showed that apoA-IV can also generate apoA-IV containing HDL particles (21). It is thus possible that apoA-IV containing HDL may fuse with apoB-48 containing particles and pull them toward the higher density regions.

LCAT corrects the aberrant HDL phenotype caused by the apoA-I[225–230] mutations

In previous studies, we have shown that naturally occurring or bioengineered point mutations in apoA-I when expressed in mouse models activate LCAT insufficiently and in some instances may lead to the accumulation of discoidal HDL particles in plasma (18, 19). Other mutations lead to very low levels of HDL cholesterol and accumulation

TABLE 2. Calculated biophysical parameters for WT apoA-I and the apoA-I [F225A/V227A/F229A/L230A] mutant

Mutation	Helicity		Thermal Denaturation			Chemical Denaturation	ANS Binding
	α -Helix	T_m ($^{\circ}$ C)	Slope ^a	Cooperativity Index (n)	$D_{1/2}$ (M)	Fold Increase ^b	
WT	59.3 ± 0.5	56.0 ± 0.5	7.8 ± 0.1	6.3 ± 0.4	1.02 ± 0.06	10.2 ± 0.5	
F225A/V227A/ F229A/L230A	51.7 ± 0.3^c	57.8 ± 0.2^d	4.0 ± 0.0^c	11.4 ± 0.4^e	1.01 ± 0.03	6.0 ± 0.4^c	

Values are means \pm SD of 3–4 experiments. Parameters obtained from the indicated measurements are as follows: α -helix is the % α -helical content of the protein as calculated from the molecular ellipticity of the protein sample at 222 nm; T_m is middle point of the thermal denaturation transition (melting temperature); slope is the calculated slope of the linear component of the thermal denaturation transition, around the melting temperature; cooperativity index n is an indicator of the cooperativity of the thermal unfolding transition and is calculated using the Hill equation $n = (\log 81) / \log(T_{0.9}/T_{0.1})$, where $T_{0.9}$ and $T_{0.1}$ are the temperatures at which the unfolding transition has reached a fractional completion of 0.9 and 0.1; $D_{1/2}$ is the guanidine HCl concentration at which the midpoint of the chemical denaturation is achieved; fold increase is the increase in ANS fluorescence in the presence of the protein relative to free ANS in the same buffer.

^a Slope is calculated from the fit of thermal denaturation curve to a Boltzman sigmoidal model curve using the equation $[\Theta]_{222} = \text{Bottom} + ((\text{Top} - \text{Bottom}) / (1 + \exp((T_m - X) / \text{Slope})))$. X describes the temperature, and slope describes the steepness of the curve, with a larger value denoting a shallow curve.

^b Fold-increase in signal compared with unbound ANS.

^c $P < 0.0001$.


^d $P < 0.05$.

^e $P < 0.001$.

of premature pre- β - and α 4-HDL particles in plasma (11). A characteristic feature of these mutations is that the low HDL levels and the abnormal HDL phenotype could be corrected in vivo by gene transfer of LCAT (11, 18, 19). The preceding article showed that substitutions of residues L218, L219, V221, and L222 by alanines led to the generation of a unique and previously undetected low HDL phenotype that was characterized by the formation of only pre- β -HDL particles and could not be converted to spherical particles by excess LCAT (8). Since the changes in the structure and the functions of the apoA-I[225–230] and the apoA-I[218–222] mutant had several similarities, we carried out experiments to determine whether the aberrant HDL phenotype generated by the apoA-I[225–230] mutations could be corrected by LCAT. These experiments showed that coexpression of the LCAT and the apoA-I[225–230] mutant in apoA-I^{-/-} mice restored the HDL cholesterol peak of the FPLC profile and shifted it toward lower densities (compare Fig. 1A with Fig. 3A). It also increased apoA-I levels and shifted its distribution to lower densities (compare Fig. 1B with Fig. 3C). Finally, it promoted the appearance of mouse apoE predominantly in the lower densities and of apoA-IV in all lipoprotein fractions (compare Fig. 1B with Fig. 3C).

Similar experiments in double-deficient mice showed that the coexpression of the LCAT and the apoA-I[225–230] mutant created a cholesterol shoulder that extended from VLDL to HDL as determined by FPLC analysis (Fig. 3B). The distribution of the mutant apoA-I, apoA-IV and apoB-48 in different densities was similar to that observed in mice expressing the apoA-I mutant alone (Fig. 3D). In both mouse models, the LCAT treatment created normal pre- β and α -HDL subpopulations and generated spherical HDL particles of a larger size. Thus, the observed LCAT insufficiency caused by the apoA-I[225–230] mutations could be reversed by treatment with LCAT.

The ability of LCAT to restore aberrant HDL phenotype caused by genetic or environmental factors may have important clinical implications for the correction of HDL abnormalities in humans. An abnormality that persisted in apoA-I^{-/-} \times apoE^{-/-} mice expressing the apoA-I[225–230] mutant was the presence of VLDL₂, IDL₂, and LDL-sized particles in the HDL fractions.

The present study in combination with the preceding study (8) shows the essential role of eight hydrophobic residues present in the 218–230 region of apoA-I for the structure and function of apoA-I and its ability to form HDL. The two studies enhance our understanding of the complex factors that contribute to the correct extracellular assembly, maturation, and proteomic composition of HDL. Future studies are required to identify by existing and new assays how the aberrant forms of HDL identified in these and previous studies (1, 2, 10, 11, 15, 18, 19) affect different functions of HDL that are required for protection from atherosclerosis and other diseases. 

Panagiotis Fotakis, Ioanna Tiniakou, and Andreas Kateifides have been students of the graduate program “The Molecular

Basis of Human Disease” of the University of Crete Medical School. The authors thank Gayle Forbes and Dr. Arnold vonEckardstein (University of Zurich) for technical assistance.

REFERENCES

1. Chroni, A., T. Liu, I. Gorshkova, H. Y. Kan, Y. Uehara, A. Von Eckardstein, and V. I. Zannis. 2003. The central helices of ApoA-I can promote ATP-binding cassette transporter A1 (ABCA1)-mediated lipid efflux. Amino acid residues 220-231 of the wild-type ApoA-I are required for lipid efflux in vitro and high density lipoprotein formation in vivo. *J. Biol. Chem.* **278**: 6719–6730.
2. Chroni, A., G. Koukos, A. Duka, and V. I. Zannis. 2007. The carboxy-terminal region of apoA-I is required for the ABCA1-dependent formation of alpha-HDL but not prebeta-HDL particles in vivo. *Biochemistry.* **46**: 5697–5708.
3. Borhani, D. W., D. P. Rogers, J. A. Engler, and C. G. Brouillette. 1997. Crystal structure of truncated human apolipoprotein A-I suggests a lipid-bound conformation. *Proc. Natl. Acad. Sci. USA.* **94**: 12291–12296.
4. Borhani, D. W., J. A. Engler, and C. G. Brouillette. 1999. Crystallization of truncated human apolipoprotein A-I in a novel conformation. *Acta Crystallogr. D Biol. Crystallogr.* **55**: 1578–1583.
5. Mei, X., and D. Atkinson. 2011. Crystal structure of C-terminal truncated apolipoprotein A-I reveals the assembly of high density lipoprotein (HDL) by dimerization. *J. Biol. Chem.* **286**: 38570–38582.
6. Ohnsorg, P. M., L. Rohrer, D. Perisa, A. Kateifides, A. Chroni, D. Kardassis, V. I. Zannis, and A. von Eckardstein. 2011. Carboxyl terminus of apolipoprotein A-I (ApoA-I) is necessary for the transport of lipid-free ApoA-I but not prelipidated ApoA-I particles through aortic endothelial cells. *J. Biol. Chem.* **286**: 7744–7754.
7. Biedzka-Sarek, M., J. Metso, A. Kateifides, T. Meri, T. S. Jokiranta, A. Muszyński, J. Radziejewska-Lebrecht, V. Zannis, M. Skurnik, and M. Jauhainen. 2011. Apolipoprotein A-I exerts bactericidal activity against *Yersinia enterocolitica* serotype O:3. *J. Biol. Chem.* **286**: 38211–38219.
8. Fotakis, P., A. Kateifides, C. Gkolfinopoulou, D. Georgiadou, M. Beck, K. Grundler, A. Chroni, E. Stratikos, D. Kardassis, and V. I. Zannis. 2013. Role of the hydrophobic and charged residues in the 218 to 226 region of apoA-I in the biogenesis of HDL. *J. Lipid Res.* Epub ahead of print. August 29, 2013; doi:10.1194/jlr.M038356.
9. Liu, T., M. Krieger, H. Y. Kan, and V. I. Zannis. 2002. The effects of mutations in helices 4 and 6 of ApoA-I on scavenger receptor class B type I (SR-BI)-mediated cholesterol efflux suggest that formation of a productive complex between reconstituted high density lipoprotein and SR-BI is required for efficient lipid transport. *J. Biol. Chem.* **277**: 21576–21584.
10. Chroni, A., H. Y. Kan, K. E. Kypreos, I. N. Gorshkova, A. Shkodrani, and V. I. Zannis. 2004. Substitutions of glutamate 110 and 111 in the middle helix 4 of human apolipoprotein A-I (apoA-I) by alanine affect the structure and in vitro functions of apoA-I and induce severe hypertriglyceridemia in apoA-I-deficient mice. *Biochemistry.* **43**: 10442–10457.
11. Koukos, G., A. Chroni, A. Duka, D. Kardassis, and V. I. Zannis. 2007. LCAT can rescue the abnormal phenotype produced by the natural ApoA-I mutations (Leu141Arg)Pisa and (Leu159Arg)FIN. *Biochemistry.* **46**: 10713–10721.
12. Luo, J., Z. L. Deng, X. Luo, N. Tang, W. X. Song, J. Chen, K. A. Sharff, H. H. Luu, R. C. Haydon, K. W. Kinzler, et al. 2007. A protocol for rapid generation of recombinant adenoviruses using the AdEasy system. *Nat. Protoc.* **2**: 1236–1247.
13. Rothblat, G. H., M. de la Llera-Moya, V. Atger, G. Kellner-Weibel, D. L. Williams, and M. C. Phillips. 1999. Cell cholesterol efflux: integration of old and new observations provides new insights. *J. Lipid Res.* **40**: 781–796.
14. Fielding, C. J., V. G. Shore, and P. E. Fielding. 1972. A protein cofactor of lecithin:cholesterol acyltransferase. *Biochem. Biophys. Res. Commun.* **46**: 1493–1498.
15. Chroni, A., H. Y. Kan, A. Shkodrani, T. Liu, and V. I. Zannis. 2005. Deletions of helices 2 and 3 of human apoA-I are associated with severe dyslipidemia following adenovirus-mediated gene transfer in apoA-I-deficient mice. *Biochemistry.* **44**: 4108–4117.
16. Zannis, V. I., E. E. Zanni, A. Papapanagiotou, D. Kardassis, and A. Chroni. 2006. ApoA-I functions and synthesis of HDL: insights

- from mouse models of human HDL metabolism. *In* High-Density Lipoproteins. From Basic Biology to Clinical Aspects. C. J. Fielding, editor. Wiley-VCH, Weinheim. 237–265.
17. Lyssenko, N. N., M. Hata, P. Dhanasekaran, M. Nickel, D. Nguyen, P. S. Chetty, H. Saito, S. Lund-Katz, and M. C. Phillips. 2012. Influence of C-terminal α -helix hydrophobicity and aromatic amino acid content on apolipoprotein A-I functionality. *Biochim. Biophys. Acta*. **1821**: 456–463.
 18. Koukos, G., A. Chroni, A. Duka, D. Kardassis, and V. I. Zannis. 2007. Naturally occurring and bioengineered apoA-I mutations that inhibit the conversion of discoidal to spherical HDL: the abnormal HDL phenotypes can be corrected by treatment with LCAT. *Biochem. J.* **406**: 167–174.
 19. Chroni, A., A. Duka, H. Y. Kan, T. Liu, and V. I. Zannis. 2005. Point mutations in apolipoprotein A-I mimic the phenotype observed in patients with classical lecithin:cholesterol acyltransferase deficiency. *Biochemistry*. **44**: 14353–14366.
 20. Timmins, J. M., J. Y. Lee, E. Boudyguina, K. D. Kluckman, L. R. Brunham, A. Mulya, A. K. Gebre, J. M. Coutinho, P. L. Colvin, T. L. Smith, et al. 2005. Targeted inactivation of hepatic Abca1 causes profound hypoalphalipoproteinemia and kidney hypercatabolism of apoA-I. *J. Clin. Invest.* **115**: 1333–1342.
 21. Duka, A., P. Fotakis, D. Georgiadou, A. Kateifides, K. Tzavlaki, L. von Eckardstein, E. Stratikos, D. Kardassis, and V. I. Zannis. 2013. ApoA-IV promotes the biogenesis of apoA-IV-containing HDL particles with the participation of ABCA1 and LCAT. *J. Lipid Res.* **54**: 107–115.